Journal of
Mechanical
Science and
Technology

Journal of Mechanical Science and Technology 21 (2007) 1008~1017

An Experimental Study on LMR Core Seismic Behavior with Fluid Couplings Between Closely Spaced Hexagons

Gyeong-Hoi Koo*, Jae Han Lee

Korea Atomic Energy Research Institute, P.O. Box 105, Yusong, Daejeon, 305-600, Korea.

(Manuscript Received September 11, 2006; Revised April 2, 2007; Accepted April 2, 2007)

Abstract

In LMR (Liquid Metal Reactor) core seismic behavior, the fluid coupling between closely spaced hexagons is known to have a very strong effect on the natural frequencies and the seismic responses. In this paper, an experimental study is carried out to investigate the fluid coupling effects with reduced scale mock-ups with three types of hexagonal duct systems and three types of input seismic motions such as the ElCentro 1940 time history, the artificial time history (Reg. 1.60), and the Kobe time history by using a one-dimensional shaking table facility. The results of the experimental studies are compared and discussed with those of the analyses performed by using the SAC-CORE code, which implements a numerical algorithm of the CFAM (Consistent Fluid Added Mass) matrix proposed in a previous paper. From the results, it is found that the fluid coupling between closely spaced hexagons becomes stronger with an increasing number of the neighboring hexagonal ducts, and this causes the natural frequency to be significantly changed and it affects the seismic time history responses too.

Keywords: Core seismic analysis; Fluid coupling; CFAM (Consistent Fluid Added Mass) matrix; FAMD code; SAC-CORE code; Liquid metal reactor

1. Introduction

To describe the complicated LMR (Liquid Metal Reactor) core seismic behavior with an appropriate mathematical model, several kinds of modeling approaches have been proposed (Horiuchi, 1991; Morishita, 1993; IAEA, 1995; 1996). The principal mathematical technique used in most modeling methods is based on the fluid added mass approach by the Fritz formula (Fritz, 1972). This method considers a core system as a co-cylinder structure filled with a fluid between the inner cylinder and the outer cylinder. The whole core assemblies become an inner cylinder as a single cluster and the core shroud becomes an outer cylinder. This method is very simple but there is a lack of a detailed description of a fluid coupling effect, especially between closely spaced duct hexagons. As is well-known in previous studies (Chen, 1976; Yang, 1980), the size of a fluid gap significantly affects the fluid coupling forces. Therefore, it is necessary to consider the fluid coupling forces between the ducts in the case of a closely spaced hexagonal core system of an LMR. To overcome a simple clustering fluid added mass approach, a new numerical application algorithm by applying the CFAM (Consistent Fluid Added Mass) matrix, which includes off-diagonal terms by considering the coupling terms between all neighboring duct hexagons, has been proposed with a simplified core seismic analysis model in a previous paper (Koo, 2004).

In this paper, an experimental study is carried out to investigate the fluid coupling effects with reduced

*Corresponding author. Tel.: +82 42 868 2950, Fax.: +82 42 861 7697
E-mail address: ghkoo@kaeri.re.kr

scale mock-ups with three types of hexagonal duct systems and three types of input seismic motions such as the ElCentro 1940 time history, the artificial time history (Reg. 1.60), and the Kobe time history by a using one-dimensional shaking table facility. To do this, three types of mock-up arrangement such as a single-Hex system, a 3-Hex system with a center row, and a 7-Hex system are experimented in air and water conditions. From the experimental results, the fluid coupling effects on the seismic time history responses and the natural frequencies are discussed for each mock-up in detail and compared with the simulation results calculated by the SAC-CORE code (Koo, 2002).

2. Descriptions of experiments

2.1 Configurations of the experimental mock-up

Figure 1 shows the configuration of the experimental mock-up used in this paper. As shown in the figure, the main body of the ducts has a uniform hexagonal section and the lower parts of the ducts are fabricated as a nosepiece with cylindrical sections that is fixed at the lower plate called the diagrid. As shown in Fig. 2, there are two types of ducts. One type is the center duct (symbol A), which has a 1.0 cm outer diameter of a nosepiece, and the other type is that surrounding the center duct, which has a 1.4 cm diameter of a nosepiece. Therefore, a more flexible center duct surrounded by six relatively stiff ducts is fabricated to be able to invoke impacts with the neighboring ducts during the seismic excitations. The full length of the duct is 70 cm including the 10 cm nosepiece and the length of the flat-to-flat is 4.1 cm. The fluid gap distance between all the ducts is 0.2 cm and the diameter of an outer cylinder containing the fluid is 32.4 cm. Actually, it is difficult to set up and adjust the gap size to be exactly 0.2 cm for all the gaps between the ducts in the experiments. Due to the sensitivity of the gap size on the seismic time history responses, the slightly misarranged gap sizes are measured and considered in the seismic response analysis.

2.2 Threet types of experimental mock-up

To investigate the fluid coupling effects between the closely space hexagonal ducts with small fluid gaps, three types of experimental mock-ups such as the 1-Hex system, the 3-Hex system, and the 7-Hex

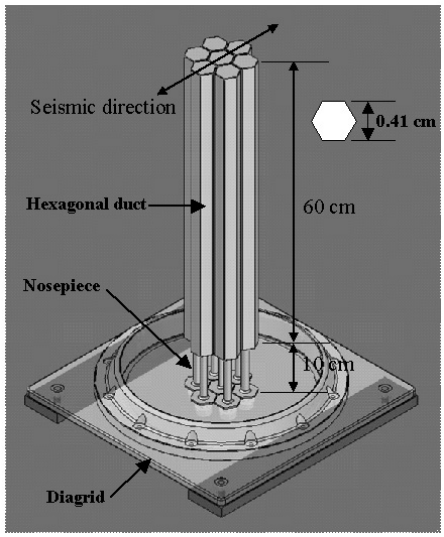

Fig. 1. Experimental core mock-up.

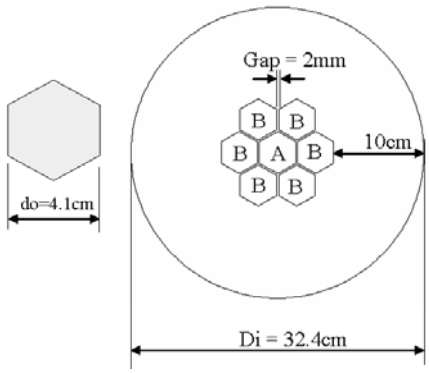

(a) Top view

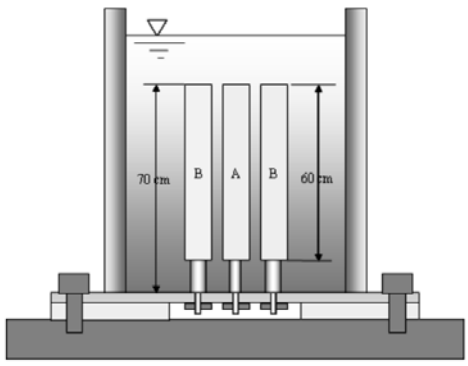

* Nosepiece Diameter :
D_A = 1.0cm, D_B = 1.4cm

(b) Front view

Fig. 2. Dimensions and arrangement of the experimental mock-up.

Table 1. Overall experimental conditions.

Experimental Type	Input Seismic Motions	Conditions
1-Hex System	- ElCentro - ATH - Kobe	In-Air
		In-Water
3-Hex System (Single-Row)	- ElCentro - ATH - Kobe	In-Air
		In-Water
7-Hex System	- ElCentro - ATH - Kobe	In-Air
		In-Water

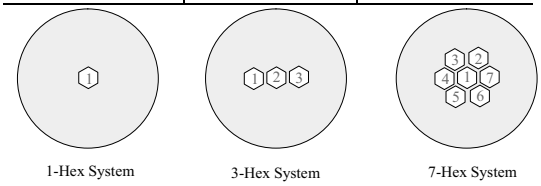

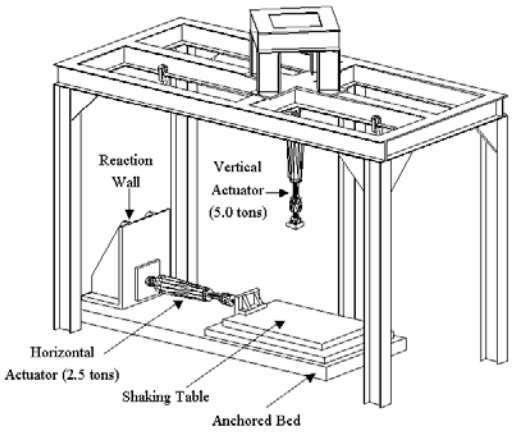

Fig. 3. Schematics of the one-directional shaking table used in the experiments.

system are used. For each mockup, three types of seismic input motions and two types of fluid conditions are experimented. Therefore, as shown in Table 1, a total of 18 types of experiments are carried out.

For the 1-Hex system, there are no closely spaced neighboring hexagons around the central duct. Therefore, this mock-up represents a one duct system submerged in an infinite confined fluid without the fluid coupling effects between the ducts. For the 3-Hex system, the central duct is closely placed between the left and right side ducts in the direction of the seismic excitation. Actually, this model is selected to be the single row model conventionally used in a core seismic analysis. For the 7-Hex system, the central duct is surrounded by six hexagons with 0.2 cm fluid gaps. The main purpose of this system is

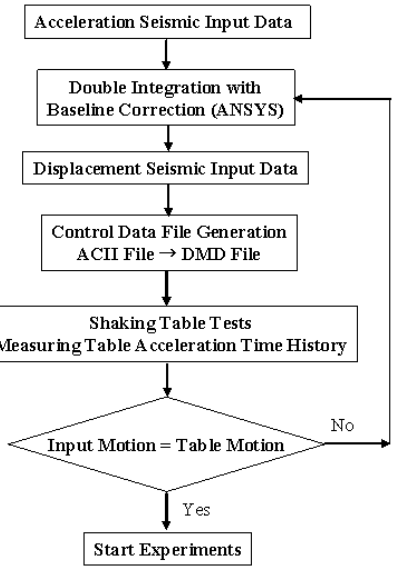

Fig. 4. Overall procedures of the experiments.

Table 2. Mechanical properties used in the analysis model.

	Elevation Top(m)	Elevation Bottom(m)	Density (1E3 kg/m^3)	Cross Sectional Area (1E-3 m^2)	Young's Modulus (1E11 Pa)	Area Moment of Inertia (1E-9 m^4)
Center Duct (C)	0.000	0.050	7.80	7.854E-2	1.9	0.491
	0.050	0.100	7.80	7.854E-2	1.9	0.491
	0.100	0.200	7.80	1.456	1.9	169.943
	0.200	0.300	7.80	1.456	1.9	169.943
	0.300	0.400	7.80	1.456	1.9	169.943
	0.400	0.700	7.80	1.456	1.9	169.943
	0.700	0.710	5.35	1.456	1.9	169.943
Outer Ducts (L & R)	0.000	0.050	7.80	0.154	1.9	1.886
	0.050	0.100	7.80	0.154	1.9	1.886
	0.100	0.200	7.80	1.456	1.9	169.943
	0.200	0.300	7.80	1.456	1.9	169.943
	0.300	0.400	7.80	1.456	1.9	169.943
	0.400	0.693	7.80	1.456	1.9	169.943
	0.693	0.700	13.00	1.456	1.9	169.943

to investigate the fluid gap effects on the fluid coupling forces between the hexagonal ducts. Furthermore, this system can be used to verify a single-row seismic analysis method including the CFAM matrix obtained from the finite element analysis for the 7-Hex system (Koo, 2004).

2.3 Generation of seismic table motions

Three types of seismic input motions such as the ElCentro (1940 El Centro earthquake), the ATH (the Artificial Time History corresponding to US NRC Reg. 1.60), and the Kobe (1995 Kobe earthquake) are used in this study. Figure 3 shows the schematic of a one-dimensional shaking table facility actuated by a SCHENK actuator (2.5 tons) with a Labtronic-8800 controller. Figure 4 shows the general procedures performed in this core seismic experiment. To generate the seismic input table motions corresponding

to the input control motions, the input acceleration seismic data is transformed to displacement seismic data through a baseline correction process. To assure correct input table motions, the feedback test procedures are performed before starting the main core seismic experiments.

Through several measurements and validations of the table motions, it is confirmed that the acceleration time history data measured on the shaking table by the accelerometer (B&K 4380) coincides with the input seismic wave motions. Figure 5 shows the verified comparison results of the displacement time history data between the input motion and the real table motion. As shown in the figure, the displacement seismic table motion acquired by the position sensor installed in the actuator is exactly coincident with that of the input motion. Therefore, it is assumed that the friction effect of the roll bearing guide type of shaking table may be neglected in the core seismic experiments.

3. Mechanical properties for core seismic analysis

The mechanical properties for the center duct and the outer ducts used in the simplified lumped mass and stiffness model are shown in Table 2. The structural damping values are extracted through the impact response tests for each input seismic motion. In this work, it is found that the mock-up used, which is a small structural damping system, reveals nonlinear structural damping characteristics depending on the maximum seismic displacement response. The structural damping values used are 0.23% for the ElCentro, 0.45% for the ATH, and 0.07% for the Kobe input seismic motions.

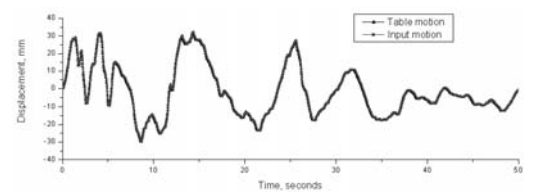

(a) Elcentro

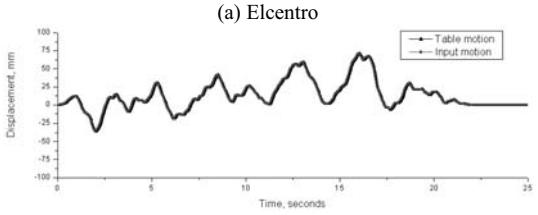

(b) ATH

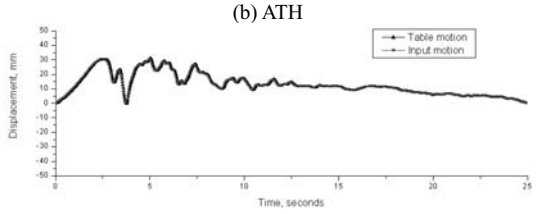

(c) Kobe

Fig. 5. Used seismic table motions.

For the modeling of the impact behavior between the closely spaced ducts, it is assumed that the impacts only occur at the top end location of the ducts and this can be modeled with the gap elements consisting of the impact spring and a damping. Since the input values of an impact stiffness and damping between the ducts may significantly affect the core seismic behavior during a seismic event, these have to be determined cautiously by experiments or analyses. In this paper, the numerical analysis method by a conventional unit stiffness finite element analysis is used for determining the impact stiffness (Koo, 2004). The impact stiffness, $\mathbf{K}_{gap}$ between the neighboring ducts can be determined simply by using both the duct stiffness values and the impact damping, and $\mathbf{C}_{gap}$ can be determined from the determined impact stiffness for the gap.

For a more detailed analysis modeling of the experimental mock-up system, the gap sizes are adjusted for each experimental mock-up, consistent with the slight changes of the fluid gap sizes occurring in the settings. These effects are also considered in the calculation of the CFAM matrix.

4. Results and discussions

4.1 Time history responses in water

Among the time history responses in the LMR core seismic behavior, the displacement seismic responses are so important from the point of view of a control rod insertion to secure the safe shutdown of a reactor and an accurate prediction of the reactivity insertion of a core during seismic excitations. Thus, the investigation of the seismic responses is focused on the displacement time history responses. In actuality, the bottom end of duct subassemblies (i.e., nosepiece) is just connected to the receptacle without any horizontal grid supports like a cantilever. It is expected that the top end of the duct reveals the maximum displacement responses during the seismic input motions. Therefore, the measurement location

of the responses is selected to be the top end of ducts.

4.1.1 For the 1-hex system

Figure 6 shows a schematic of the experimental mock-up for the 1-Hex system and its seismic analysis model. To obtain the CFAM matrix for a single hexagonal system submerged in a fluid, a finite element analysis model for a fluid field is used as shown in Fig. 6(c). Table 3(a) presents the calculated CFAM matrix by using the FAMD code (Koo, 2003). In this table, the symbols "OL" and "OR" indicate the left and right sides of the outer cylinder containing the fluid, respectively, and the symbol "C" means the central duct. This model is a very simple one without an interaction of the neighboring ducts. The off-diagonal terms in the CFAM matrix are not effective for the seismic responses. Therefore, the fluid will act like a lumped added mass on the hexagonal duct. Figures 7 and 8 show the seismic displacement time history responses at the top location in the water condition by the experiments and the analyses, respectively. When comparing these results for each seismic input motion, we can see that the analysis results are in very good agreement with those of the experiments for the maximum response values and the whole time history responses due to no complex fluid coupling with the neighboring ducts.

4.1.2 For the 3-hex system

Figure 9 shows the schematic of the experimental mock-up for the 3-Hex system and its simplified seismic analysis model, which is arrayed in the direction of the seismic input motion. In setting the experimental mock-up in the water condition, the measured gaps are slightly changed to be 3.2 mm for gap-2 and 3.5 mm for gap-3, respectively. To obtain the CFAM matrix for this model, the finite element analysis model is used as shown in Fig. 9(c). As shown in Table 3(b), the fluid added mass per unit length of the central duct itself is 2.74 kg which is larger than 1.72 kg of the 1-Hex system due to the small fluid gaps between the closely spaced adjacent ducts. The fluid added mass per unit length of the outer duct L itself is 2.23 kg, which is slightly larger than 2.18 kg of the outer duct R due to the different gap sizes. Figure 10 shows the displacement time history responses at the top of the central duct by the experiments. From the results, we can see that the seismic responses of the central duct in the case of the 3-Hex system are significantly different from those of the 1-Hex system (Fig. 7). From the time history responses, it is shown that the overall peak dis-

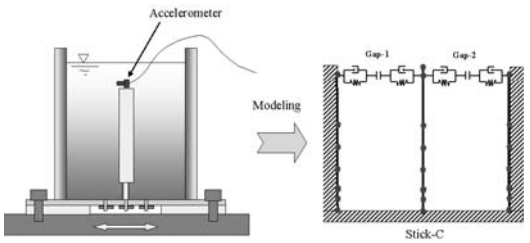

(a) Experimental mock-up (b) Seismic analysis model

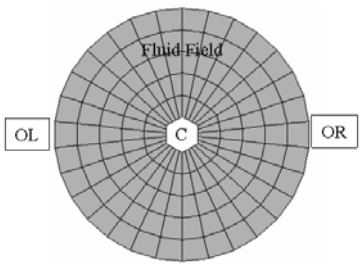

(c) CFAM analysis model

Fig. 6. Analysis model for the 1-hex system.

Table 3. Calculated CFAM matrix for each system (kg/m).

	OL	C	OR
OL	86.0	-3.75	86.0
C	-3.75	1.72	-3.75
OR	86.0	-3.75	86.0

(a) For the 1-hex system

	OL	L	C	R	OR
OL	90.5		Symmetry		
L	-2.68	2.23			
C	-1.91	-1.15	2.74		
R	-2.68	-0.05	-1.15	2.18	
OR	90.5	-2.68	-1.91	-2.68	90.5

(b) For the 3-hex system

	C	4	R	2	1	L	3	OL
C	7.18							
4	0.37	3.73				Symmetry		
R	-3.09	0.85	5.02					
2	0.37	0.35	0.82	3.73				
1	0.37	0.01	-0.72	-2.15	3.73			
L	-3.09	-0.72	-0.76	-0.72	0.85	5.02		
3	0.37	-2.15	-0.72	0.01	0.35	0.82	3.73	
OL	-4.10	-4.24	-3.06	-4.24	-4.24	-3.06	-4.24	113.0

(c) For the 7-hex system

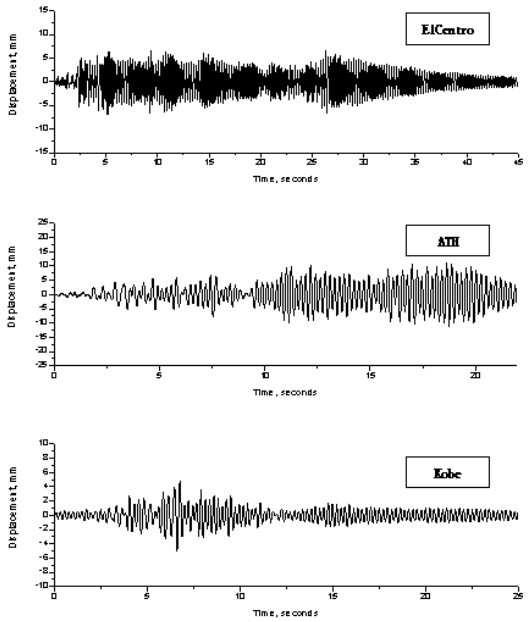

Fig. 7. Displacement responses for the 1-hex system by experiments in water.

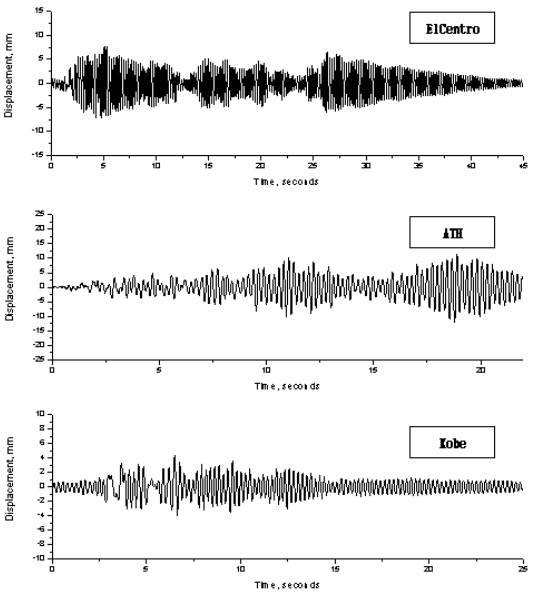

Fig. 8. Displacement responses for the 1-hex system by analyses in water.

placements of the central duct are relatively smaller than those of the 1-Hex system due to the fluid coupling effects. However, we can see that the impacts occur between the central duct and the neighboring ducts at early time points of around 2.3 to 3.2 seconds for an example of the ElCentro input

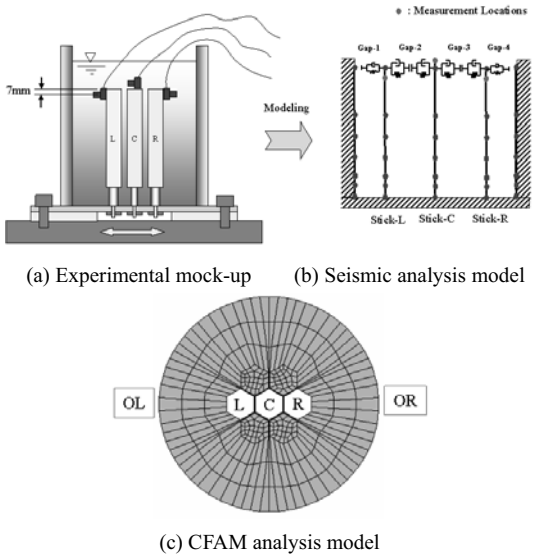

(a) Experimental mock-up (b) Seismic analysis model

(c) CFAM analysis model

Fig. 9. Analysis model for the 3-hex system.

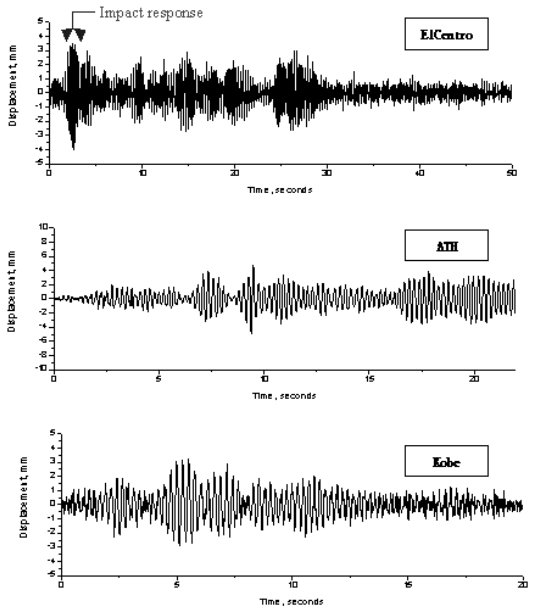

Fig. 10. Displacement responses for the 3-hex system by experiments in water.

motion. Figure 11 shows the analysis results. As shown in the figure, the analysis results show a good agreement with the experimental results over the whole time history wave motion and the maximum displacement responses throughout the seismic input types.

Figure 12 shows the analysis results of the impact responses in the air and water conditions for the ElCen-

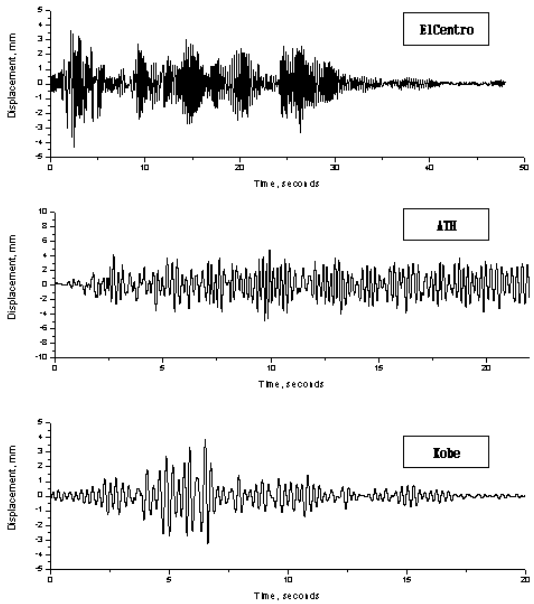

Fig. 11. Displacement responses for the 3-hex system by analyses in water.

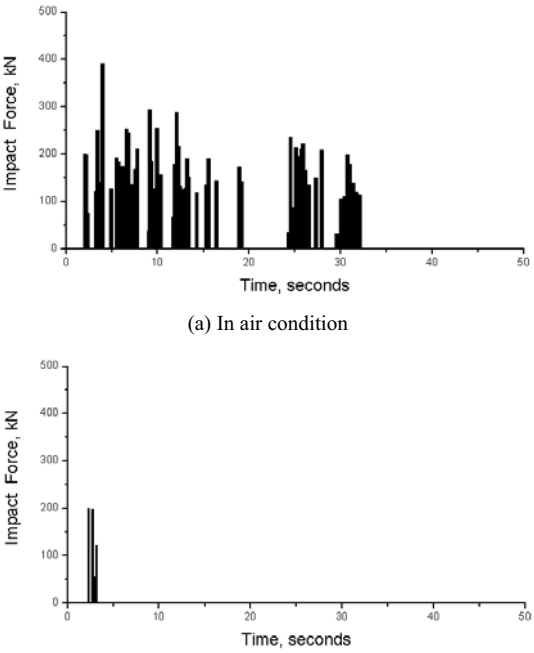

(a) In air condition

(b) In Water Condition

Fig. 12. Impact responses for the 3-hex system by analyses for the ElCentro input.

tro input motion. As shown in the figure, there are severe impacts in the air condition during a whole seismic motion, while the impacts in the water condition only occur for the early time points as mentioned in the above paragraph.

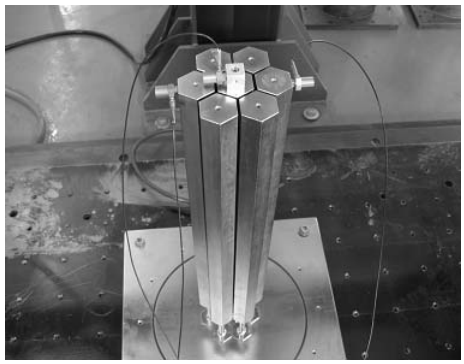

(a) 7-hex system in air

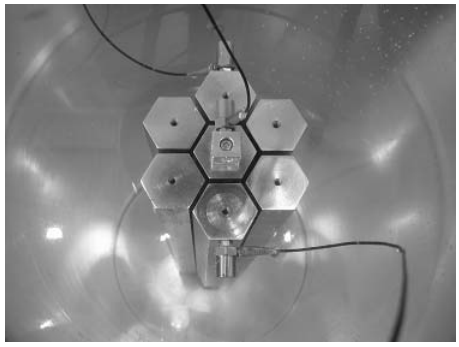

(b) 7-hex system in water

Fig. 13. Photos of the 7-hex system used in the experiments.

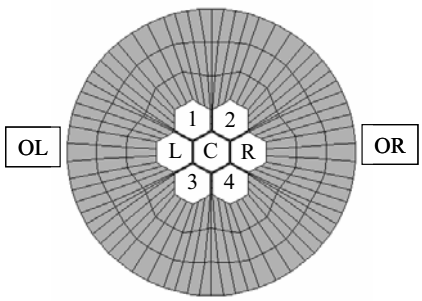

Fig. 14. Fluid coupling analysis model for the 7-hex.

4.1.3 For the 7-hex system

The seismic analysis model for the 7-Hex system is the same as that of the 3-Hex system except for the CFAM matrix in the water condition. Figure 13 exhibits the real photos of the 7-Hex system setting on the shaking table in air and water.

To obtain the CFAM matrix for this model, a fluid coupling analysis is carried out with the detailed finite element model shown in Fig. 14. The measured fluid

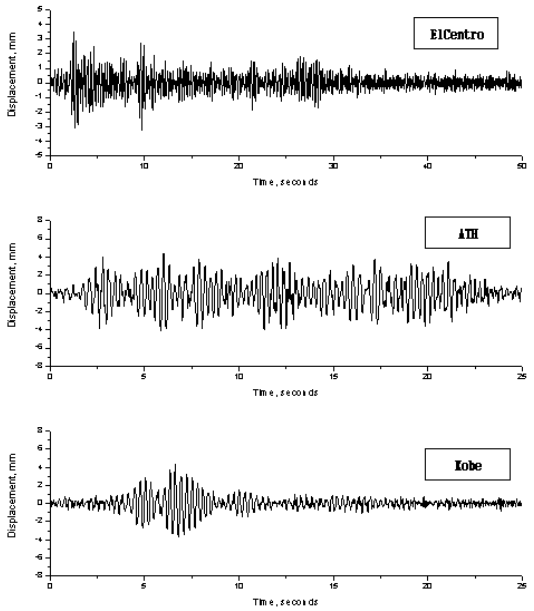

Fig. 15. Displacement responses for the 7-hex system by experiments in water.

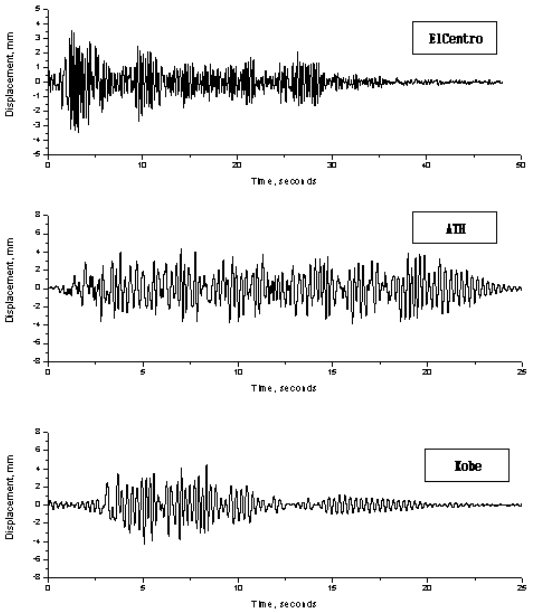

Fig. 16. Displacement responses for the 7-hex system by analyses in water.

gap sizes are the same as those of the 3-Hex system. Table 3(c) presents the calculated CFAM matrix for all the ducts and the cylinder containing the fluid. As shown in the table, the fluid added mass per unit length of the central duct C itself is 7.18 kg, which is a 260 % increase when compared with 2.74 kg of the

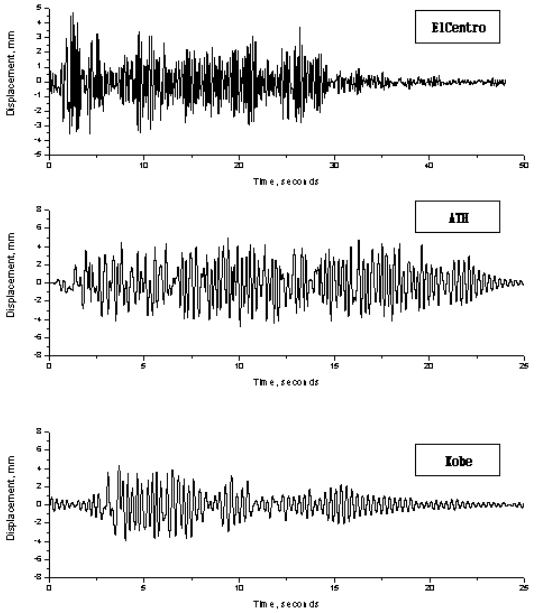

Fig. 17. Displacement responses for the7-hex system by analyses without the off-diagonal fluid coupling terms.

3-Hex system. This means that the six hexagonal ducts surrounding the central duct with small gaps invoke a significant fluid coupling and cause the CFAM matrix of the central duct to increase. Furthermore, the CFAM matrix of the outer ducts of L and R also increase when compared with those of the 3-Hex system due to the effects of the additional adjacent ducts. When investigating the off-diagonal fluid coupling terms in Table 3(c) related with the central duct, it is found that the fluid coupling masses between the ducts of the central row (L, C, R) and the off-ducts (1, 2, 3, 4) are relatively small when compared with those between the ducts of a single row (L, C, R). Therefore, the CFAM matrix for a single row model can be selected from all the results in Table 3(c) and it can be used in a simplified seismic analysis model for the 7-Hex system with a more detailed fluid coupling consideration than the conventional methods.

Figures 15 and 16 show the displacement time history responses of the central duct for each seismic input motion by the experiments and analyses, respectively. From the results, we can observe a distinctive impact behavior throughout the time history responses. When comparing the analysis results with the experimental results, it can be confirmed that the proposed simplified seismic analysis model with the fluid coupling of the CFAM

matrix can predict the nonlinear core seismic behavior well including the severe impacts of the hexagonal duct system submerged in a fluid. To investigate the effects of the off-diagonal terms in the CFAM matrix, seismic analyses are carried out without the off-diagonal terms in the CFAM matrix. As shown in the analysis results of Fig. 17, this analysis method results in overestimated seismic responses when compared with those of the experiments. This result is consistent with a previous study (Koo, 2004).

4.2 The maximum displacements

Table 4 summarizes the comparison results of the maximum displacement values obtained by the experiments and the analyses for all kinds of experiments. As shown in the results, the maximum responses in the air condition are larger than those of the in-water condition for the ElCentro and the ATH input motions. But for the Kobe input motion, the maximum displacement responses are larger in the water condition than in the air condition for all the mock-up systems. It is surmised that the lower natural frequency in the water condition may be well tuned with the Kobe input motion, which contains relatively lower excitation frequency components.

Figure 18 shows the experimental results of the maximum displacement values versus the intensities of the ElCentro seismic input load in the water condition. In the case of the 7-Hex system, the maximum seismic displacement values significantly increase as the seismic loads increase, but in the case of the 3-Hex system, the changes of the maximum displacements of the central duct are small when compared with those of the 7-Hex system.

4.3 Vibration modal characteristics

Figure 19 shows the fluid coupling effects on the natural frequencies obtained by the experiments and the analyses in the air and water conditions. As shown in the figure, the fundamental natural frequency of the central duct is 4.64 Hz in air by the experiment. It decreases to 4.35 Hz for the case of the in-water condition (1-Hex system). When there are adjacent

Table 4. Summary of the maximum displacement responses.

	ElCentro (mm)		ATH (mm)		Kobe (mm)	
	Test	**Analysis**	**Test**	**Analysis**	**Test**	**Analysis**
1-Hex (In-Air)	8.89	9.10	14.70	14.58	3.37	3.12
1-Hex (In-Water)	6.88	7.69	11.14	12.12	4.99	4.25
3-Hex (In-Air)	3.23	2.90	4.60	4.00	2.15	3.28
3-Hex (In-Water)	4.00	4.35	4.96	4.94	3.21	3.85
7-Hex (In-Air)	4.38	4.13	5.31	5.99	3.54	3.63
7-Hex (In-Water)	**3.50**	**3.54**	**4.38**	**4.38**	**4.32**	**4.39**

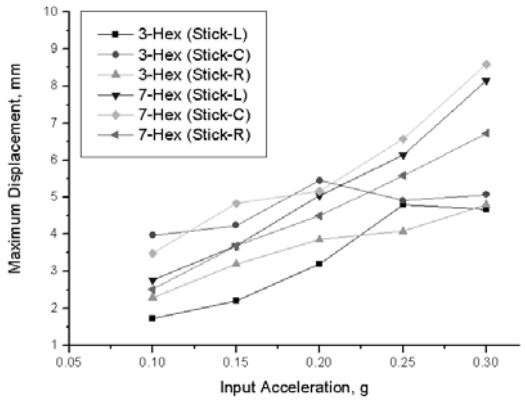

Fig. 18. Maximum displacement vs input seismic levels by the experiments in water.

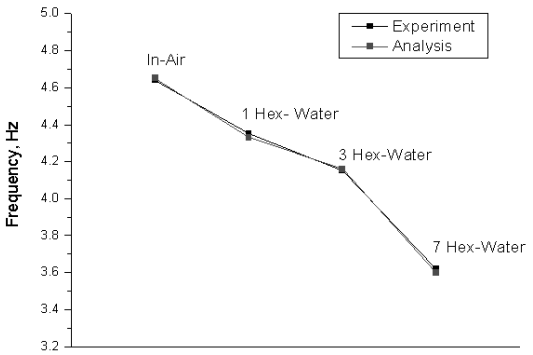

(a) For central duct

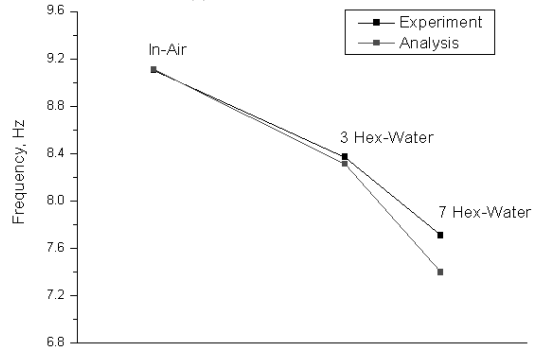

(b) For outer duct

Fig. 19. Fluid coupling effects on the natural frequencies.

ducts such as the 3-Hex system in water, the natural frequency of the central duct steadily decreases to 4.15 Hz. However, for the case of the 7-Hex system for which the central duct is surrounded by six adjacent hexagonal ducts, the natural frequency significantly decreases to 3.62 Hz. It is the same for the outer duct. This means that the fluid coupling effects increase as the number of the neighboring hexagonal ducts increases with small gaps, and it can significantly affect the vibration modal characteristics of the core system. To conclude, this experimental result clearly shows the reason why a detailed consideration of the fluid coupling effects is required in the LMR core seismic analysis method.

5. Conclusions

In this paper, the experimental study to investigate the LMR core seismic behavior was carried out to verify the core seismic analysis method with the fluid-structure coupling effects between closely spaced hexagonal duct assemblies. From the experimental studies with various mock-up types and the input motions carried out in this paper, it is shown that a fluid coupling between closely spaced hexagons becomes stronger with an increasing number of neighboring ducts. It causes a change of the natural frequencies and affects the seismic time history responses. Thus, it is strongly recommended that the CFAM matrix of the fluid coupling forces between closely spaced hexagonal ducts be obtained by a detailed finite element analysis and included in the core seismic analysis model to assure accurate core seismic analysis results.

Acknowledgment

This work has been carried out under the Nuclear R&D Program by MOST in Korea.

References

1995, "Intercomparison of Liquid Metal Reactor Seismic Analysis Codes, Volume 1: Validation of Seismic Analysis Codes Using Reactor Core Experiments," IAEA-TECDOC-798, IAEA.

1995, "Intercomparison of Liquid Metal Reactor Seismic Analysis Codes, Volume 2: Verification and Improvement of Reactor Code Seismic Analysis Codes Using Core Mock-up Experiments," IAEA-TECDOC-829, IAEA.

1996, "Intercomparison of Liquid Metal Reactor Seismic Analysis Codes, Volume 3: Comparison of Observed Effects with Computer Simulated Effects on Reactor Codes from Seismic Disturbances," IAEA-TECDOC-882, IAEA.

Chen, S. S. and Chung, H, 1976, "Design Guide for Calculating Hydrodynamic Mass," ANL-CT-76-45, ANL.

Cook, R. D., Malkus, D. S. and Plesha, M. E., 1989, "Concepts and Applications of Finite Element Analysis," Third Edition, John Wiley & Sons.

Fritz, R. J., 1972, "The Effect of Liquids on the Dynamic Motions of Immersed Solids," *Journal of Engineering for Industry, Transactions of the ASME*, pp. 167~173.

Horiuchi, T., Nakagawa, M. and Ohashi, M., 1991, "Fluid Structure Coupled Vibration Characteristics of FBR Core Components," *Proc. 11th Int'l. Conf. on SMiRT*, Vol. E, 381.

Koo, G. H. and Lee, J. H., 2002, "Development of SAC-CORE2.0 for Core Seismic Analysis," KAERI/TR-2312/2002, KAERI.

Koo, G. H. and Lee, J. H., 2003, "Development of FAMD Code to Calculate the Fluid Added Mass and Damping of Arbitrary Structures Submerged in Confined Viscous Fluid," *KSME International Journal*, Vol. 17, No. 3, pp.457~466.

Koo, G. H. and Lee, J. H., 2004, "Fluid Effects on the Core Seismic Behavior of a Liquid Metal Reactor," *KSME International Journal*, Vol. 18, No. 12, pp. 2125~2136.

Morishita, M. and Iwata, K, 1993, "Seismic Behavior of a Free Standing Core in a Large LMFBR," Nuc. Eng. Des., Vol. 140, pp. 309~318.

Yang, C. I. and Moran, T. J., 1980, "Calculations of Added Mass and Damping Coefficients for Hexagonal Cylinders in a Confined Viscous Fluid," *Journal of Pressure Vessel Technology*, Vol. 102, pp. 152~157.